Heartbeat and Respiration Detection Using a Low Complexity CW Radar System

Panagiota Kontou[1*], Souheil Ben Smida[1], Spyridon Nektarios Daskalakis[1*], Symeon Nikolaou[2], Mauro Dragone[1], Dimitris E. Anagnostou[1]

[1]Institute of Sensors, Signals and Systems (ISSS), Heriot-Watt University, Edinburgh, UK

[2]Frederick Research Center, Nicosia, Cyprus

[*]{pk44, sd70}@hw.ac.uk

***Abstract* — Cardiopulmonary monitoring mainly relies on electrodes in contact with the skin. This can be challenging in cases of patients with compromised skin, premature babies or in assisted living applications where the elderly may remove their sensors. Hence, it is of high importance to be able to detect human vital signs in a contactless and non-intrusive manner. Methods such as the use of cameras do not protect the privacy of a patient. This work presents the theory and optimized implementation of an alternative method, a continuous wave (CW) radar sensor system, that successfully detects the heartbeat and respiration of a person from a distance of 1 m. The proposed implementation allows for the first time, to improve the quality of the detected signal by cancelling undesired DC components, detrimental to heartbeat detection via manual analog tuning.**

***Keywords* — cardiopulmonary, healthcare, heartbeat, medical radar, microwave, noncontact sensing, respiration, vital signs.**

I. Introduction

Radar systems had been developed mostly to determine distance from an aircraft or to measure the speed of a vehicle by measuring the frequency or phase shift of the reflected signal [1]. However, microwave radars have been used to detect vital signs monitoring, since the 1970s [2].

Traditional respiration and heart rate measurement methods require to be in contact with the patient which is uncomfortable and does not allow for continuous monitoring. Reliable contactless devices, such as radars, could be clinically valuable in the prognosis of a disease and monitoring until full recovery, especially in cases such as patients with compromised skin and sleep monitoring [2].

Peak-to-peak chest displacement due to respiration is about 4-12 mm, whereas heartbeat causes a displacement of around 0.5 mm according to [3]. Chest displacement of 1 cm results in 1 radian (57.6°) of phase change using a frequency signal of 2.4 GHz. This results in phase variation related to respiration between 23° and 69° that is easily detectable [2] – [9]. However, the phase variation that is related to heartbeat is less than 3°.

Thus, it is very important to have a high-performance Doppler effect demodulator, to be able to discriminate between respiration and heartbeat. Moreover, any Doppler effect reception suffers from the null points problem, and one way to avoid this is to use a quadrature demodulator [4].

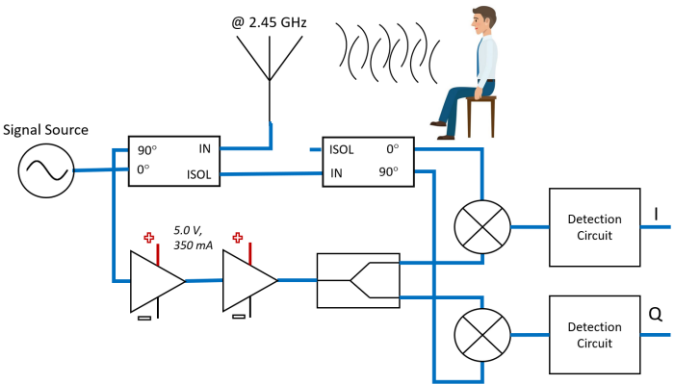

Fig. 1. Block diagram of the proposed CW radar-based system for heartbeat detection.

State-of-the-art systems reported reliable respiration and heartbeat measurements by using high carrier frequency [5], complex detection circuits that perform DC cancellations [6], and advanced signal processing algorithms [7], [8] to alleviate the problem stated above.

In work [9], a mathematical analysis is presented and a prototype system, demonstrating the effectiveness of arctangent demodulation in quadrature receivers. By modifying the structure proposed in [9], this paper proposes a radar-based system operating at a 2.4 GHz ISM band that uses quadrature (I/Q) receiver, range correlation effect and DC offset elimination method. This work provides a simpler, low complexity hardware implementation resulting in a lower cost future design.

II. CW Radar for Healthcare Monitoring

A. System Theory

A CW radar system for respiration and heartbeat detection was developed using a homodyne transceiver architecture, as shown in Fig. 1. A continuous wave (CW) signal $T(t)$ with frequency 2.4 GHz is emitted via a transmitting (TX) antenna. The CW can be defined as:

$$T(t) = A_T \cdot \cos(2\pi f t), \qquad (1)$$

where f is the carrier frequency and A_T the amplitude.

The subject's chest wall movement $x(t)$, which comes from the respiration and heartbeat, modulates the RF signal

and part of it is reflected to the radar system. The total distance travelled is $2d(t) = 2d_0 + 2x(t)$, where d_0 is the average distance between the subject and the radar. The signal received by the receiving (RX) antenna of the radar can be defined as:

$$R(t) = A_R \cdot cos\left[2\pi f\left(t - \frac{2d(t)}{c}\right)\right], \quad (2)$$

where c is the signal's propagation velocity. As the carrier wavelength is given by $\lambda = {}^{c}/_{f}$, (2) can be modified to (3):

$$R(t) = A_R \cdot cos\left[2\pi ft - \frac{4\pi d_0}{\lambda} - \frac{4\pi x(t)}{\lambda}\right]. \quad (3)$$

Comparing (1) and (3), it is clear that the received signal resembles the transmitted one with an added time delay that depends on the distance of the subject. This time delay is modulated by the periodic chest movement of the subject. The received signal can be demodulated by mixing it with a local oscillator (LO) circuit. If the LO input of the mixer comes from the same source as the transmitted, the received signal is downconverted to baseband and possible transmit and receive phase noises are cancelled out in the baseband signal. This is called range correlation effect as described in work [4]. The baseband signal at the output of the mixer is given by:

$$B(t) = \cos\left[\theta + \frac{4\pi x(t)}{\lambda}\right], \quad (4)$$

where θ is the constant phase shift which depends on the nominal distance d_0.

B. Demodulation Method

As can be seen from (4), signal $x(t)$ is modulated in the cosine function. Small angle approximation is used when θ is an odd multiple of $\pi/2$. In the case where θ is an even multiple of $\pi/2$, the baseband output is not proportional to chest displacement, therefore it cannot be determined. In this case, a "null point" occurs. Null points are generated when the LO and the received signal are in-phase or 180° out-of-phase and appear every $\lambda/4$ from the radar, which for a 2.4 GHz signal will be 3 cm.

To find the optimum points by changing the position of the subject or the system would be impractical and would likely lead to incorrect measurements. A quadrature receiver would improve the performance of the system, as at least one output will be in the optimum point. In this case the radar system will include two receiver chains in phase (I) and quadrature (Q), with two LO circuits working independently and having phase difference $\pi/2$.

In reality, *I/Q* signals are not pure sine waves, but according to [9], there is an added DC offset that is generated by the reflections of the stationary objects in the room and various circuit flaws, such as the mixers self-mixing, and cannot be predicted. The baseband outputs are described as:

$$B_I(t) = A_I \cdot \cos\left(\theta_0 + \frac{4\pi x(t)}{\lambda}\right) + DC_I, \quad (5)$$

$$B_Q(t) = A_Q \cdot \sin\left(\theta_0 + \frac{4\pi x(t)}{\lambda}\right) + DC_{Q,} \quad (6)$$

with DC_I and DC_Q being the DC offset terms.

III. CW Radar Based System Implementation

A. System Hardware

To validate the theoretical results, a prototype of the radar was designed in Heriot-Watt University Electromagnetics Lab. The design was based in the schematic of Fig. 1 and the prototype of the radar system is depicted in Fig. 2.

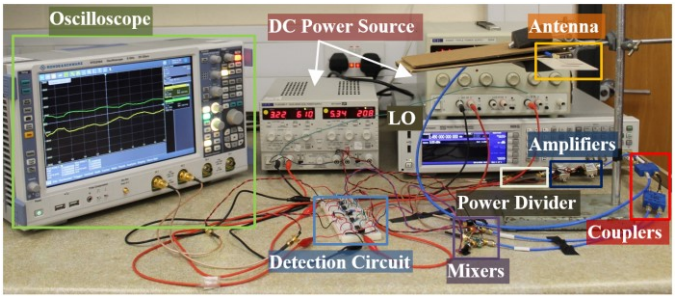

Fig. 2. Implementation of CW radar-based system according to the block diagram of Fig. 1.

As it is depicted in the schematic of Fig. 1, the design consists of a signal generator that generates the 2.45 GHz CW with a power of 3 dBm, two mixers, two couplers, two low noise amplifiers (LNAs), a power divider and two detection circuits. The LO phase is 0° in one mixer and 90° in the other mixer (quadrature demodulator). The radar system includes only one end-fire microstrip antenna and specifically, a compact planar *Yadi-Uda* antenna for transmitting and receiving the signals. The antenna has a resonant frequency at 2.45 GHz and gain of 6dBi in free space.

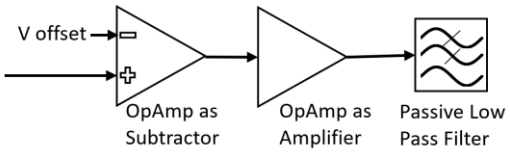

Fig. 3. Detection circuit to manually tune the signal so that DC offsets can be removed.

The detection circuit of this system is described in Fig. 3 and it is much simpler than the one used in [9]. The output signals of the mixers are described by (5) and (6). The fundamental frequencies of heartbeat and respiration are very close to DC (0.1-2.5 Hz), which and the I/Q outputs can be calibrated to remove the DC offsets. In this work, this is achieved using two operational amplifiers (LM741) for every circuit and the signal is manually tuned to eliminate the DC offsets. The signal is then amplified to obtain a wider dynamic range and is filtered with a passive low-pass filter in order to remove the high frequency components.

The main components of the radar proof-of-concept implementation is described in Table 1. The table provides all the blocks names, the models, and the specifications of every block. A laboratory power supply was used for powering the low noise amplifiers (LNAs), the mixers and the detector circuits.

Table 1. Blocks of the proposed CW radar-based system.

Block	Model	Specifications
Signal Generator	Keysight MXG N5183B	2.45 GHz; Pout: 3 dBm
Mixers	Analog Devices LTC5549	2 - 14 GHz
Couplers	Anaren Model 10016-3	2 - 4 GHz
LNA	Mini-Circuits ZX60-V63+	0.05 - 6 GHz; Gain: 20 dB
Antenna	Planar *Yadi-Uda*	2.45 GHz; Gain: 6dBi

B. Experimental Results

Measurements were carried out to one volunteer, who was standing in front of the antenna and was breathing normally, as depicted in Fig. 4. Varying the distance from 0.25 to 1 m between the antenna and the volunteer, data were recorded for about 40 s with a sampling frequency of 1 kHz. An oscilloscope (Rohde & Schwarz RTO2064) was used for the capturing and visualization of the I/Q output signals. The I/Q outputs were imported in Matlab for further processing. The volunteer was using a wearable fitness tracker to record the heartbeat as a reference. The breaths taken in the measurements were counted by the volunteer.

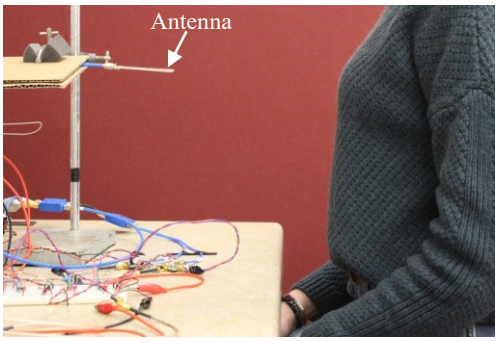

Fig. 4. Measurement setup for CW radar system: volunteer is seated at a distance of 25 cm, facing the antenna and breathing normally.

Fig. 5 shows a capture of raw I/Q measurement data for 40 s with sampling frequency 1 kHz and 0.5 m distance between the antenna and the volunteer. Each rise in the signal of the I channel indicates an inhale and each fall indicates an exhale.

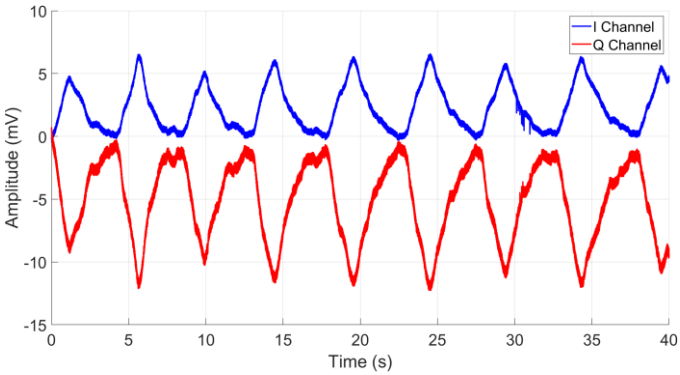

Fig. 5. Raw *I* and *Q* data capture for 0.5 m distance between the antenna and the volunteer.

The received signal was processed, and unwrapped phase of the complex envelope was taken. After that the phase was smoothed by taking the median over a twenty-element sliding window. The phase signal is shown in Fig 6. It can be observed that there is a phase change from 21° to 32°, which corresponds to the theoretical phase change for breathing stated in the introduction. Small phase changes from 1° to 3° are also visible, which is also expected according to theory.

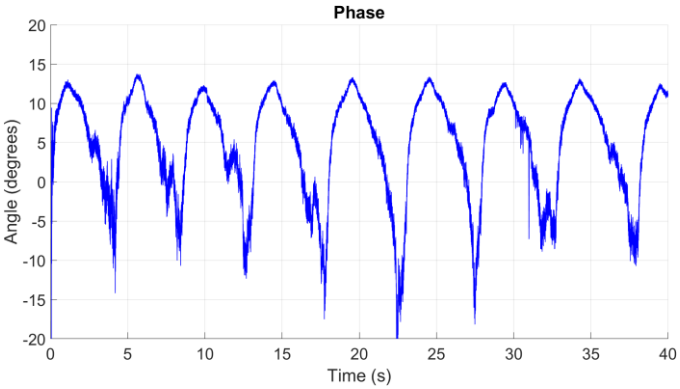

Fig. 6. Unwrapped phase of the received signal.

Fast Fourier transform (FFT) is applied to the complex envelope and the unwrapped phase of the received signal. The FFT results can be seen in Fig 7. For this measurement, the heart rate of the volunteer according to the wearable fitness tracker was about 89 beats per minute (bpm). This is 1.48 beats per second (Hz), which is one of the spikes observed in the FFT. The highest peak was observed at 0.212 Hz, which is the breathing frequency, since approximately 8.5 breaths were taken in 40 seconds. In Fig. 7, it can be observed that both signals have identical spikes in 0.2 Hz and 1.48 Hz.

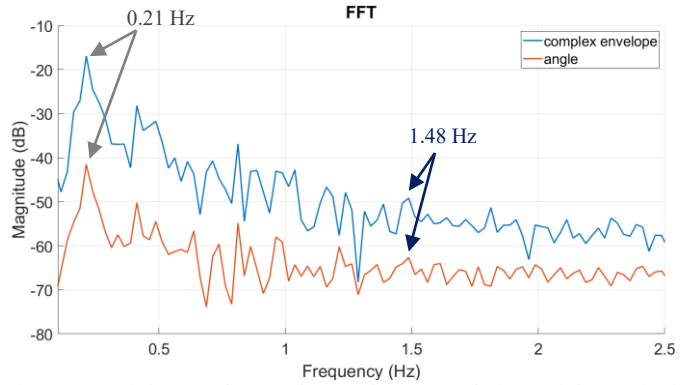

Fig. 7. FFT of the complex envelope and unwrapped phase of the received signal.

To recover the heartbeat and respiration, the inverse FFT (IFFT) was applied to the complex envelope of the received signal keeping only the frequencies between 0.1-0.5 Hz for respiration and the frequencies between 1-30 Hz for heartbeat. Fig. 8 shows the heartbeat signal of this measurement. When zooming in 0-10 s, 14 peaks can be observed, which results in 14 heartbeats in 10 s, thus, 89 bpm. The radar measurement results are positively correlated with the fitness tracker measurement.

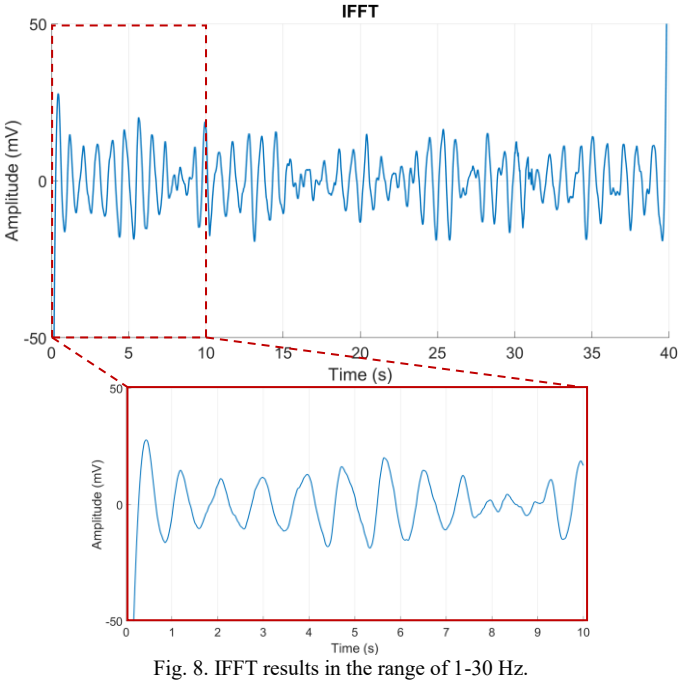

Fig. 8. IFFT results in the range of 1-30 Hz.

Fig. 9 shows the IFFT signal in frequencies between 0.1-0.5 Hz. This area corresponds to the respiration signal of this measurement. The frequency of the signal corresponds to the counted breaths taken.

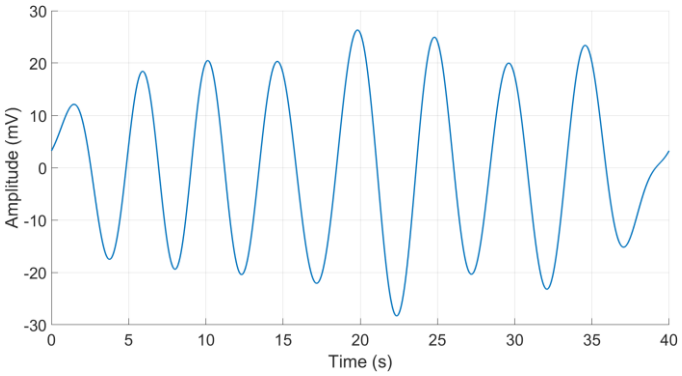

Fig. 9. IFFT results in the range of 0.1-0.5 Hz where the respiration frequency is, that shows the respiration pattern of this measurement.

IV. Conclusion

In this work, a proof-of-concept radar-based system for human health monitoring is described. The low-cost measurement unit can successfully detect heartbeat and respiration from a varying distance of 25 cm to 1 m. Future research includes comparing the measurements with the wearable fitness tracker and ECG recording for multiple volunteers. Additionally, future work will focus on automation of the tuning system, further signal processing techniques including machine learning to predict the expected heart pattern and compare with the received one to detect possible medical conditions as they occur.

Acknowledgment

This research was partially funded by the European H2020 Marie Skłodowska-Curie Individual Fellowship (MSCA-IF) grant #840854 (VisionRF) and by the Cyprus RIF, RESTART 2016-2020 EXCELLENCE/1216/376 (SWITCH).

References

[1] M. I. Skolnik, "Radar handbook", *McGraw-Hill Professional*, ISBN: 0070579083, 1970.

[2] J. C. Lin, "Noninvasive microwave measurement of respiration", *Proceedings of the IEEE,* vol. 63 Is. 10, 1975, pp. 1530-1530.

[3] O. Boric-Lubecke, V. M. Lubecke, A. D. Droitcour, B.-K. Park, and A. Singh, "Doppler radar physiological sensing", *Wiley Online Library*, 2016.

[4] A. D. Droitcour, O. Boric-Lubecke, V. M. Lubecke, J. Lin and G. T. Kovacs, "Range correlation and I/Q performance benefits in single-chip silicon Doppler radars for noncontact cardiopulmonary monitoring", *IEEE Transactions on Microwave Theory and Techniques*, vol. 52, Is. 3, 2004, pp. 838-848.

[5] C. Li and J. Lin, "Random body movement cancellation in Doppler radar vital sign detection", *IEEE Transactions on Microwave Theory and Techniques*, vol. 56, Is. 12, 2008, pp. 3143-3152.

[6] C. Y. Hsu, C. Y. Chuang, F. K. Wang, T. S. Horng and L. T. Hwang, "Detection of vital signs for multiple subjects by using self-injection-locked radar and mutually injection-locked beam scanning array", In *2017 IEEE MTT-S International Microwave Symposium (IMS)*, 2017, pp. 991-994.

[7] M. C. Huang, J. J. Liu, W. Xu, C. Gu, C. Li, and M. Sarrafzadeh, "A self-calibrating radar sensor system for measuring vital signs", *IEEE Transactions on Biomedical Circuits and Systems*, vol. 10, Is. 2, 2015, pp. 352-363.

[8] W. Xu, C. Gu, C. Li, and M. Sarrafzadeh, "Robust Doppler radar demodulation via compressed sensing", *Electronics Letters*, vol. *48, Is.* 22, 2012 pp. 1428-1430.

[9] B.-K. Park, O. Boric-Lubecke and V. M. Lubecke, "Arctangent demodulation with DC offset compensation in quadrature Doppler radar receiver systems", *IEEE Transactions on Microwave Theory and Techniques*, vol. 55, Is. 5, 2007, pp.1073-1079.